**CETRA**[2026] 27-30 May 2026, Bol, Island Brač, Croatia
**9th International Conference on Road and Rail Infrastructure**

# A UNIFIED FRAMEWORK FOR MECHANISTIC CORRELATION BETWEEN LABORATORY AND FIELD RUTTING RESPONSE IN ASPHALT PAVEMENT

**Suhas Thyagatur Ramachandraiah, Surya Marimuthu, Krishna Prapoorna Biligiri**
*Department of Civil and Environmental Engineering, Indian Institute of Technology Tirupati, Tirupati, Andhra Pradesh India*

## Abstract

Accurate prediction of rutting performance in flexible pavements necessitates understanding the relationship between laboratory performance tests, numerical simulations, and actual field behavior. Although the repeated load permanent deformation-flow number (RLPD-FN) test is widely used to evaluate rutting resistance, its direct applicability to field performance remains uncertain. Thus, the objective of study was to integrate experimental, computational, and field-scale data that helped develop a unified framework for establishing a correlation between laboratory-field rutting responses. RLPD-FN tests were conducted on dense-graded asphalt mixtures using standard protocols, and the permanent strain rate with respect to loading cycles was used to characterize the onset of tertiary flow. To complement the experimental work, three-dimensional (3D) finite element (FE) multilayered flexible pavement system was modeled in ABAQUS®, which incorporated viscoplastic constitutive models calibrated using the laboratory stress-strain responses. Further, field validation was performed using the in-situ vertical compressive strain ($\varepsilon_v$) collected from an instrumented National Highway in India, where pavement response was recorded under real-time traffic loading using embedded strain gauges. The simulation environment replicated test conditions, including confinement, loading waveform, and boundary constraints, thus enabling the capture of $\varepsilon_v$ evolution. The numerical RLPD-FN was determined based on the strain-rate inflection criterion consistent with laboratory practice. Field strain accumulation patterns were processed to derive an equivalent field RLPD-RLPD-FN, enabling direct comparison with laboratory and simulated RLPD-FN magnitudes. A correlation framework was then developed to relate RLPD-FN obtained from the laboratory, FE simulations, and in-situ $\varepsilon_v$. Essentially, the correlations between the controlled laboratory testing and complex field behavior using ABAQUS® simulations was rational. Overall, the integrated methodology provided a robust approach in translating laboratory rutting performance to field conditions and supporting reliable pavement performance predictions, thus providing a potential framework for incorporation in the mechanistic design guidelines of flexible pavement systems.

*Keywords: asphalt mixtures, flow number, finite element simulations, in-situ strains, laboratory-field correlation*

## 1 Introduction

Rutting or permanent deformation is one of the most prevalent distresses in flexible pavements worldwide attributed to the accumulation of irreversible strains within the asphalt surface wearing course and underlying unbound layers [1, 2]. The deformation in asphalt mixtures mainly occurs in three stages: primary, secondary, and tertiary, of which the transition from secondary to tertiary stage indicates the rapid increase in permanent strain that causes accelerated rutting failure [3]. Therefore, accurately predicting the initiation of critical deformation and implementing timely preventive maintenance are essential in ensuring the long-term performance of asphalt pavements [4]. In this direction, several laboratory test methods are available to evaluate various stages of permanent deformation, including the Hamburg Wheel Tracking Test (HWTT), Asphalt Pavement Analyzer (APA), Flow Time (FT) test, Repeated Load Permanent Deformation–Flow Number (RLPD-FN) test, and the |E*| dynamic modulus test [5, 6]. However, owing to the potential in capturing the three stages of permanent deformation, the RLPD-FN test has received significant attention from researchers worldwide as a primary method for characterizing the rutting potential of asphalt mixtures [7].

Further, in actual field conditions, flexible pavements are subjected to various traffic loadings that result in progressive accumulation of permanent strains within the pavement structure [8]. Significantly, the finite element (FE) modeling of multilayered pavement systems offers a means to investigate the stages of permanent deformation in asphalt layers and underlying unbound layers, also under realistic traffic loading conditions. In addition to the aforementioned laboratory-based tests, numerous three-dimensional (3D) FE models have therefore been developed to analyze the structural responses of flexible pavements and these numerical models were also employed to capture the impact of traffic loading on the progression of permanent deformation [9-11]. A recent study evaluated the permanent deformation behavior, which adopted 3D FE modeling of multilayered pavement system and quantified the influence of traffic loading and material on the accumulation of vertical compressive strains ($\varepsilon_v$) in the asphalt concrete layer and subgrade [12]. However, the importance of viscoplastic model parameters used to comprehend the permanent deformation was recognized after incorporating the field-calibrated material properties such as the |E*| dynamic modulus and viscoplastic model parameters extracted from the RLPD-FN tests into the 3D FE pavement models capable of capturing the failure stages of the asphalt mixture [13, 14].

In a nutshell, the various efforts underscored the potential use of 3D FE pavement models in mechanistic interpretation of the laboratory-derived viscoplastic model parameters and in evaluating the strain evolution under realistic boundary conditions. Although the |E*| dynamic modulus and RLPD-FN tests have demonstrated strong agreement during laboratory evaluations, the existing studies have not established a clear relationship between laboratory results and field rutting performance of the pavement system. Thus, the objective of the study was to integrate experimental, computational, and field-scale data to help develop a unified framework that establishes a correlation between laboratory-to-field rutting responses. The scope of the effort encompassed (figure 1):

- extraction of field-cored asphalt specimens from the newly constructed National Highway (NH) and pavement instrumentation
- laboratory experimentation program to obtain viscoplastic model parameters
- development of a 3D FE pavement model, validated using the instrumented in-situ pavement response data
- simulation of axle load to predict deformation in asphalt layers and subgrade
- establishment of a framework for correlating laboratory and field rutting responses.

It is envisioned that the developed FE framework will assist in evaluating the rutting damage in the asphalt pavement caused by axle and vehicle-specific loads, leading to the development of mechanistic design guidelines of flexible pavement systems.

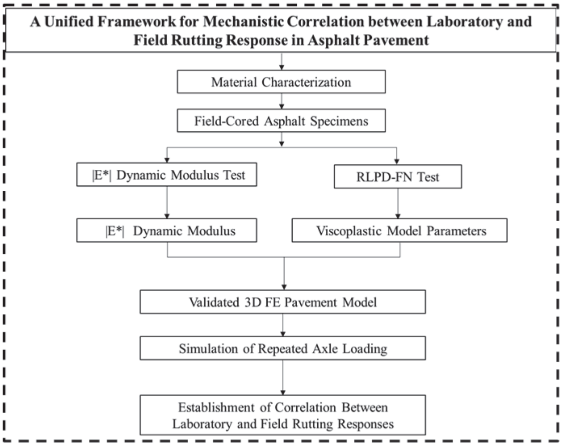


**Figure 1** Research framework

## 2 Pavement instrumentation and laboratory experimental program

National Highway-71 (NH-71), spanning 58 km between Renigunta and Naidupeta, India, which serves as a vital freight corridor in southern India was selected for full-scale pavement instrumentation due to its high ambient temperatures and heavy traffic. The flexible pavement section consisted of Bituminous Concrete (BC-I), Dense Bituminous Macadam (DBM-II), Wet Mix Macadam (WMM), Cement Treated Base (CTB), Granular Sub-Base (GSB), and subgrade. A 10 m × 5 m test area across three lanes was instrumented with 30 sensors: 13 horizontal strain gauges, 13 vertical strain gauges, 2 earth pressure cells, and 2 temperature sensors, as shown in figures 2a and 2b. Vertical strain gauges were placed at each layer interface to measure εv related to rutting, while horizontal strain gauges were positioned at BC-DBM and DBM-WMM interfaces to capture tensile strains ($\varepsilon_t$) relevant to fatigue. Earth pressure cells monitored dynamic stresses at DBM-WMM and WMM-CTB interfaces, while temperature sensors captured asphalt thermal gradients affecting viscoelastic behavior. Installation was performed layer-by-layer, ensuring sensor protection. Amongst all instruments, vertical strain gauges yielded the most reliable data, making them the primary input for validating the 3D FE pavement model. To incorporate the pavement material properties into the 3D FE pavement system, BC-I and DBM-II cylindrical specimens of 150 mm diameter and 110 mm height were cored and extracted from the instrumented NH section, as displayed in figure 3.

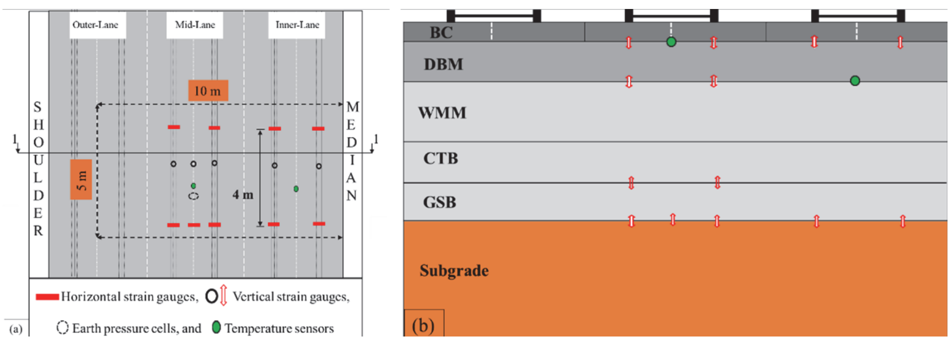


**Figure 2** Instrumented pavement section: a) plan showing placement of gauges, b) cross-section at 1-1 showing vertical strain gauges and temperature sensors


**Figure 3** Field-cored specimens: a) extraction, b) thickness measurement

## 2.1 |E*| dynamic modulus test

The |E*| dynamic moduli of field-cored specimens were obtained at -10, 4.4, 21.1, 37.8, and 54.4 °C, and across 25, 10, 5, 1, 0.5, and 0.1 Hz, following the standard test procedure [15]. Also, the experimental setup encompassed three linear variable differential transducers (LVDT) positioned 120° apart, as shown in figure 4a. Further, to characterize the time-temperature dependency of dynamic modulus of asphalt mixtures, |E*| master curves were constructed for the BC-I and DBM-II mixtures using the time-temperature superposition principle at a reference temperature of 21.1 °C [7], as presented in figure 4b.

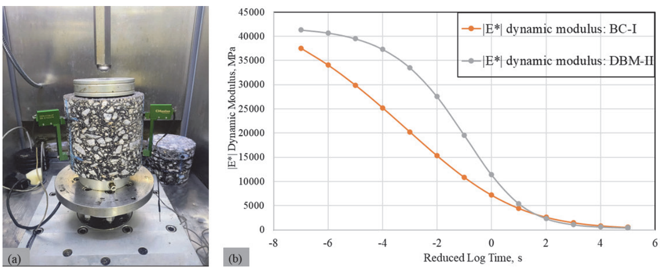


**Figure 4** |E*| Dynamic modulus test: a) experimental setup with three LVDTs (third LVDT not seen), b) actual |E*| master curves

## 2.2 Repeated load permanent deformation-flow number (RLPD-FN) test

RLPD-FN tests were performed on the field-cored specimens at three deviatoric stress levels: 0.4, 0.5, and 0.6 MPa in accordance with the established procedure [6]. Figure 5 presents the RLPD-FN experimental setup and evolution of the accumulated permanent strain (με) as a function of load cycles (N) under repeated loading at any deviatoric stress. Note that the stress level of 0.5 MPa was used for repeated loading in FE model, while all the three stress levels were used in extracting the viscoplastic model parameters, as discussed next.

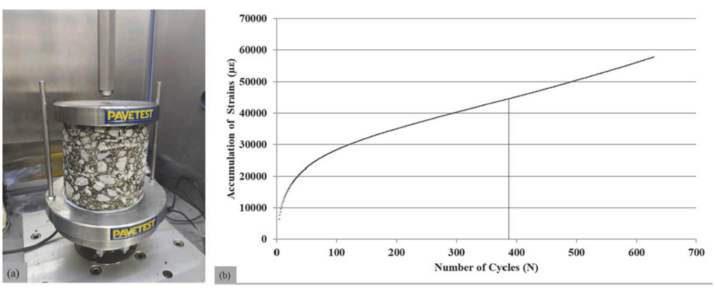


**Figure 5** RLPD-FN test: a) experimental setup for RLPD-FN, b) strain variation with number of cycles (N)

The response exhibited characteristic viscoplastic deformation behavior typically observed in asphaltic materials subjected to cyclic stress. At the initial stage of loading (N < ~80 cycles), the material illustrated a rapid increase in permanent strain representing the primary region of creep. Further, the response transitioned into a secondary region, characterized by a near-linear relationship between permanent strain and load cycles (approximately $100 \leq N \leq 390$). To characterize the stress-dependent viscoplastic behavior of the asphalt mixture, a time-hardening power law creep model was adopted. The constitutive relationship implemented in this study was expressed using the equation (1) [16]:

$$\varepsilon_{cr} = A\, \sigma^{n}\, t^{m} \tag{1}$$

Where, $\varepsilon_{cr}$ is creep strain rate, σ is stress component, t is time, and A, n, m are the creep power law parameters of asphalt mixtures. The model parameters were optimized using nonlinear regression analysis of the secondary stage obtained from the RLPD-FN testing conducted at multiple stress levels. The optimized magnitudes of the creep power law parameters were determined as follows: $A = 8.2\times10^{-4}$; $n = 1.758$; and $m = 1.2\times10^{-2}$.

## 2.3 3D FE pavement model development

A 3D FE pavement model was developed in ABAQUS® whose dimensions were set to 3.5 m (longitudinal, x-direction) × 1.3 m (vertical, y-direction) × 7 m (transverse, z-direction) in accordance with the literature [17, 18]. The FE model replicated the full-scale NH asphalt pavement section with actual layer thicknesses and materials (figure 6a), discretized using C3D8R eight-node brick elements. A friction coefficient of 0.5 was assigned at layer interfaces with hard normal contact, and boundary conditions restricted lateral movement while fixing the bottom to simulate rigid support. Axle loading was applied as a single axle dual wheel (SADW) with a 360 cm² circular contact area (10.7 cm radius per wheel), and dynamic implicit analysis captured the time-dependent response. It is noteworthy that the asphalt layers (BC-I and DBM-II) were modeled using the time-hardening viscoplastic creep power law with calibrated parameters [13] in ABAQUS®. Figures 6a and 6b depict the model cross-section, material properties, loading area, and meshing of the pavement system that subjected to FE analysis.

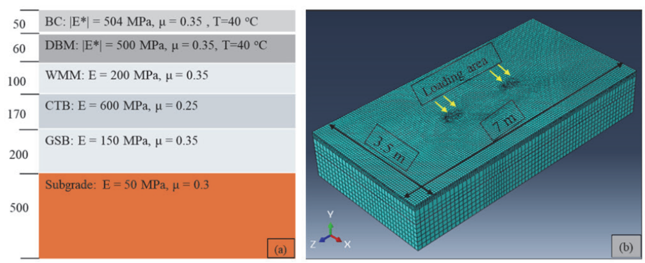


**Figure 6** 3D FE model of NH pavement section: a) field cross-section and material properties (depth, mm), b) 3D FE model geometry and mesh of the pavement system

## 2.4 3D FE pavement model validation

The accuracy and reliability of the developed 3D FE pavement model were evaluated through the predicted responses and validated against field measurement data obtained from the instrumented pavement section, as presented in figure 7a. Further, the validation focused on comparing in-situ $\varepsilon_v$ (figure 7b) measured in the bituminous layers and subgrade with the corresponding strains predicted by the 3D FE pavement model.

The comparison revealed a strong agreement between the FE predictions and field data, confirming the capability of the 3D FE pavement model that replicated the structural response of the pavement system under dynamic traffic loading.

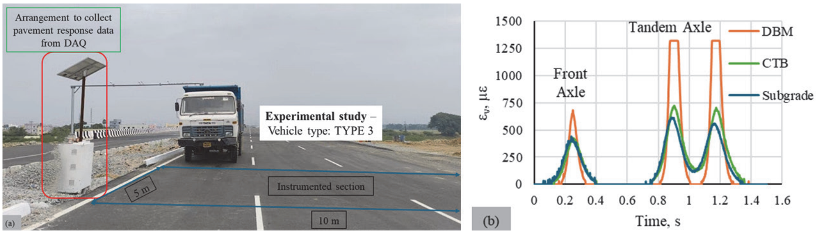


**Figure 7** Instrumented pavement section: a) vehicle type used for experimental study, b) response of pavement system at 20 km/h

Furthermore, figures 8a and 8b present the layer-wise comparison of the predicted and observed in-situ $\varepsilon_v$, particularly for asphalt and subgrade layers, respectively. Figure 8c illustrates the spatial distribution of pavement strains using a contour plot under transient loading conditions. Thus, the time-history analysis demonstrated a good agreement in both trend and magnitude of $\varepsilon_v$ between the field observations and FE predictions.

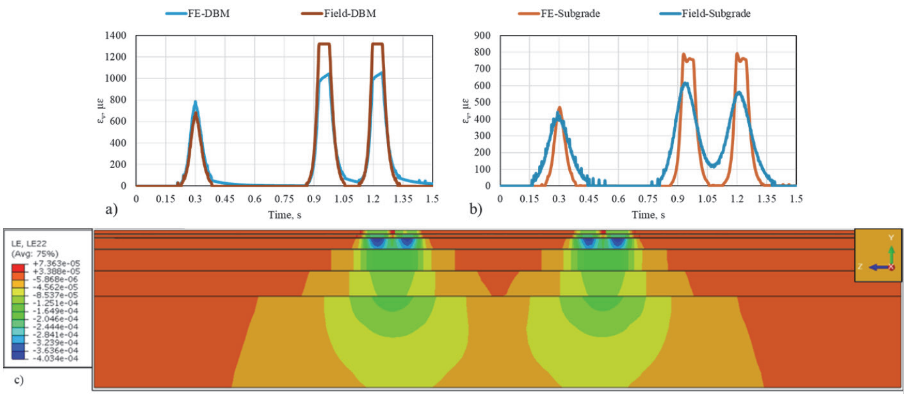


**Figure 8** 3D FE pavement model and field responses: a) strain-time histories below asphalt layer, b) strain histories on subgrade top, c) strain contour across pavement layers in FE model

## 3 Results and discussion

The pavement responses were evaluated by applying a repeated axle load of 0.5 MPa, consistent with the stress level adopted in the laboratory RLPD-FN test, as shown in figure 9a. The predicted permanent deformation response demonstrated a progressive accumulation of strain with increasing load cycles, as displayed in figure 9b. The strain-cycle relationship exhibited a continuously increasing trend without abrupt discontinuities, indicating stable viscoplastic deformation during the initial loading phase. The RLPD-FN obtained from the laboratory test was observed at 392 loading cycles with strain observed around 44,500 με, indicating the onset of tertiary flow under the applied stress condition. In contrast, the multilayered pavement model predicted a vertical strain of approximately 44,500 με at 75,000 loading cycles without exhibiting an abrupt failure-type transition within the simulated cycle range. Thus, the substantial difference in the number of cycles reflected the distinction between material-level instability observed with the laboratory RLPD-FN testing and the structural response of the layered pavement system under distributed loading conditions.

Further, at 75,000 cycles, the computed subgrade strain was approximately 693 με, which was significantly lower than the vertical strain in the asphalt layer.

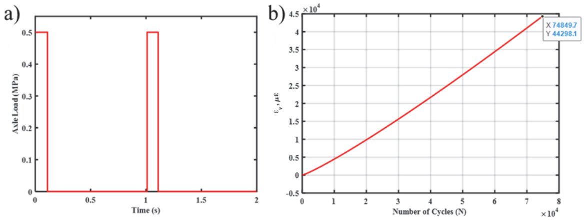


**Figure 9** FE analysis: a) applied pressure history of 0.5 MPa, b) strain variation of asphalt layer with number of loading cycles (N)

The 3D FE pavement model illustrated the spatial distribution of strains within the multilayer pavement system subjected to a repeated axle load of 0.5 MPa, as presented in figure 10. The strain contour indicated that most of the strains were concentrated within the asphalt layer, while the underlying subgrade experienced comparatively moderate strain accumulation. The results therefore suggested that although the asphalt mixture exhibited flow instability at relatively low loading cycles during the laboratory testing, the multilayer pavement system redistributed stresses effectively, thus delaying excessive strain accumulation at the structural level. Furthermore, the contour plots clearly demonstrated the development of localized high-strain zones directly beneath the wheel contact areas, remarking that concentrated load transfer occurred via the asphalt layer and then into the underlying structural layers. However, the presence of elevated strain concentrations directly beneath the contact area indicated that the asphalt layer experienced dominant viscoplastic deformation under repeated loading.

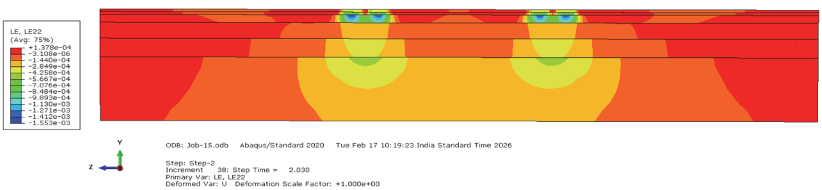


**Figure 10** Vertical strain contour across the pavement layers

## 4 Conclusion

The major objective of the study was to integrate experimental, computational, and field-scale data that helped develop a unified framework in establishing a correlation between the laboratory-to-field rutting responses. Based on the study findings, the major conclusions and recommendations included: Laboratory characterization and 3D FE viscoplastic modeling of pavement system: The RLPD-FN test effectively captured the viscoplastic instability behavior of the asphalt mixtures through identification of tertiary flow using the minimum strain-rate criterion. Multi-stress RLPD-FN data enabled calibration of a time-hardening power law creep model, accurately representing nonlinear permanent strain accumulation. The laboratory-derived viscoplastic model parameters were incorporated into a 3D FE pavement model that could integrate the viscoplastic constitutive behavior. The FE simulations effectively reproduced strain evolution under realistic dual-wheel axle loading and multilayer boundary conditions.

Correlation of laboratory-to-field rutting responses: A substantial difference was observed between the laboratory RLPD-FN (RLPD-FN = 392 cycles at 0.5 MPa) and the load repetitions predicted by the 3D FE pavement system to reach comparable vertical strain levels (~75,000 cycles), highlighting the fundamental difference between confined material-level instability and distributed structural-level response in a multilayer pavement system. The incorporation of laboratory-calibrated viscoplastic model parameters within the validated 3D FE model enabled mechanistic translation of laboratory-defined tertiary flow into structural response under realistic axle loading and boundary conditions. The FE simulations demonstrated that permanent deformation was predominantly concentrated within the asphalt layers, while subgrade strains remained comparatively moderate, confirming effective stress redistribution and structural confinement in a flexible pavement system.
Recommendations: Pavement design framework must incorporate strain-based mechanistic translation of laboratory RLPD-FN results into structural-level performance indicators rather than directly adopting laboratory FN as empirical design thresholds. The so-developed approach enabled accurate prediction of rutting progression by accounting for multilayered stress redistribution, viscoplastic strain accumulation, and realistic axle loading boundary conditions within a 3D FE framework. Although the analysis was conducted under controlled stress levels and constant loading frequency analogous to the laboratory RLPD-FN conditions, it is envisioned that the study will pave the way toward developing an advanced mechanistic design framework that would integrate temperature-dependent behavior, variable traffic spectra, and long-term strain evolution to quantify rutting in asphalt and subgrade layers, eventually leading to the establishment of performance-based mechanistic pavement design guidelines.

## References


[1] Erlingsson, S.: Rutting development in a flexible pavement structure, Road Mater. Pavement Des., 13 (2012) 2, pp. 218–234, DOI: 10.1080/14680629.2012.682383

[2] Liu, G.: Rutting prediction models for asphalt pavements with different base types based on RIOHTrack full-scale track, Constr. Build. Mater., 305 (2021), 124793

[3] Zhou, F., Scullion, T.: Discussion: Three stages of permanent deformation curve and rutting model, Int. J. Pavement Eng., 3 (2002) 4, pp. 251–260, DOI: 10.1080/1029843021000083676

[4] Liu, Z.: Rutting prediction of asphalt pavement with semi-rigid base: numerical deling on laboratory to accelerated pavement testing, Constr. Build. Mater., 375 (2023), 130903

[5] Walubita, L.F., Fuentes, L., Lee, S.I., Dawd, I., Mahmoud, E.: Comparative evaluation of five HMA rutting-related laboratory test methods relative to field performance data: DM, FN, RLPD, SPST, and HWTT, Constr. Build. Mater., 215 (2019), pp. 737–753, DOI: 10.1016/j.conbuildmat.2019.04.250

[6] Zhang, J., Alvarez, A.E., Lee, S.I., Torres, A., Walubita, L.F.: Comparison of flow number, dynamic modulus, and repeated load tests for evaluation of HMA permanent deformation, Constr. Build. Mater., 44 (2013), pp. 391–398

[7] Witczak, M.W., et al.: Simple performance test for Superpave mix design, National Academy Press, Washington, DC United States, 2002.

[8] Chen, X., Zhang, J., Wang, X.: Full-scale field testing on a highway composite pavement dynamic response, Transp. Geotech., 4 (2015), pp. 13–27

[9] Elseifi, M.A., Al-Qadi, I.L., Yoo, P.J.: Viscoelastic modeling and field validation of flexible pavements, J. Eng. Mech., 132 (2006) 2, pp. 172–178, DOI: 10.1061/(ASCE)0733-9399(2006)132:2(172)

[10] Hu, X., Zhong, S., Walubita, L.F.: Three-dimensional modelling of multilayered asphalt concrete pavement structures: strain responses and permanent deformation, Road Mater. Pavement Des., 16 (2015) 3, pp. 727–740, DOI: 10.1080/14680629.2015.1028968

[11] Cheng, H., Wang, Y., Liu, L., Sun, L.: Effects of using different dynamic moduli on predicted asphalt pavement responses in mechanistic pavement design, Road Mater. Pavement Des., 23 (2022) 8, pp. 1860–1876, DOI: 10.1080/14680629.2021.1924842

[12] Assogba, O.C., Sun, Z., Tan, Y., Nonde, L., Bin, Z.: Finite-element simulation of instrumented asphalt pavement response under moving vehicular load, Int. J. Geomech., 20 (2020), 04020006, DOI: 10.1061/(ASCE)GM.1943-5622.0001616

[13] Shanbara, H.K., Ruddock, F., Atherton, W.: A viscoplastic model for permanent deformation prediction of reinforced cold mix asphalt, Constr. Build. Mater., 186 (2018), pp. 287–302, DOI: 10.1016/j.conbuildmat.2018.07.127

[14] Saevarsdottir, T., Erlingsson, S.: Modelling of responses and rutting profile of a flexible pavement structure in a heavy vehicle simulator test, Road Mater. Pavement Des., 16 (2015), pp. 1–18, DOI: 10.1080/14680629.2014.939698

[15] Pellinen, T.K., Witczak, M.W., Bonaquist, R.F.: Asphalt mix master curve construction using sigmoidal fitting function with non-linear least squares optimization, Recent Advances in Materials Characterization and Modeling of Pavement Systems, 2012, pp. 83–101, DOI: 10.1061/40709(257)6

[16] Kim, Y.R., Lee, Y.C., Lee, H.J.: Correspondence principle for characterization of asphalt concrete, J. Mater. Civ. Eng., 7 (1995) 1, pp. 59–68, DOI: 10.1061/(ASCE)0899-1561(1995)7:1(59)

[17] Barriera, M., Lebental, B., Pouget, S.: Towards road pavement response under moving loads, Road Mater. Pavement Des., 20 (2019), S480–S499, DOI: 10.1080/14680629.2019.1588780

[18] Karimi, M.N., Mallick, R.B.: Flexible pavement instrumentation: a state-of-the-art review, J. Transp. Eng. Part B Pavements, 149 (2023), 03123001, DOI: 10.1061/JPEODX.PVENG-1175